LAWRENCE
LIVERMORE
NATIONAL
LABORATORY

LLNL-CONF-432901

Cross-magnetic-field drift algorithms and results for edge-plasma transport

S. K. Nam, T. D. Rognlien

May 21, 2010

Plasma Surface Interaction Conference
San Diego, CA, United States
May 24, 2010 through May 28, 2010

P2-62

Cross-magnetic-field drift algorithms and results for edge-plasma transport

S.K. Nam[*] and T.D. Rognlien

Lawrence Livermore National Laboratory, Livermore, CA 94551 USA

Abstract

Simulation of 2D edge transport in the tokamak pedestal-gradient and scrape-off layer regions typically show substantially slowed or lack-of convergence to steady state when ExB, ∇B, and curvature drift terms are included for steep H-mode profiles. Thus, improvement of the robustness and accuracy of edge transport codes with drifts is a high priority, and even more so as these codes become components within integrated whole-device models. Recently, Rozhansky *et al*. proposed a new numerical formulation of the drift terms and show that there is an improvement in the SOLPS code performance and accuracy, though an artificial stabilizing diffusive term is still required beyond the physical turbulent diffusive term. Here results from UEDGE implementation of the new B2SOLPS5.2 algorithm are compared to the original UEDGE and UEDGE with B2SOLPS5.0 algorithms. The new algorithms are used to simulate the DIII-D discharge in the H-mode regime.

PACS: 52.30.Ex, 52.55.-s, 52.55.Rk, 52.65.-y

JNM keywords: Mathematical and Computational Methods, Theory and Modelling

PSI-19 keywords: B2/EIRENE, Cross-Field Transport, Edge modeling, Edge plasma, UEDGE

**Corresponding author address:* LLNL, L-630, 7000 East Ave, Livermore, CA 94551 USA

**Corresponding and Presenting author E-mail:* nam3@llnl.gov

Presenting author: Sang Ki Nam

1. Introduction

Inclusion of E×B, ∇B, and curvature drift terms in 2D edge plasma transport codes typically results in substantially slower convergence or lack of convergence for obtaining steady-state profiles. Those cases where convergence is obtained show that drifts can have strong effect of the scrape-off layer plasma profiles and flows, and thus improvement of the efficiency and robustness of edge transport codes with drifts is a high priority, especially as these codes become components within integrated whole-device models. V. Rozhansky *et al.* have proposed a new numerical formulation of the drift terms, and it is shown to improve the B2SOLPS code performance and accuracy, though an artificial stabilizing diffusive term is still required beyond the physical diffusive term [1]. Though the fully implicit algorithm in UEDGE requires no separate stabilizing term, the artificial diffusive term is implemented into UEDGE and the performance is compared with the original UEDGE and UEDGE with the new formulation of B2SOLPS.

2. Simulation model for perpendicular drifts

Since the divergence-free convective fluxes give zero contribution to the conservation equations [2], it is best to omit those terms from the outset to improve numerical accuracy [3]. The separation of particle fluxes into divergence-free terms and those from guiding-center motion is clearly reviewed by Chankin [4]. The divergence-free term, so called magnetization flux is given by [4]

$$\begin{aligned}\nabla\times\vec{K} &= \frac{1}{eB^2}\vec{B}\times\nabla p-\frac{2p}{eB^3}\vec{B}\times\nabla B-\frac{p}{eB^2}\nabla\times\vec{B}\\ &=\nabla\times\left(\frac{-p}{eB^2}\vec{B}\right).\end{aligned} \tag{1}$$

So the ∇p drift, which is the pressure-driven drift, so called diamagnetic drift, can be replaced by the ∇B drift avoiding the numerical difficulty in calculating the steep gradient of the pressure especially in H-mode.

$$\frac{1}{eB^2}\vec{B}\times\nabla p = \nabla\times\vec{K} + \frac{2p}{eB^3}\vec{B}\times\nabla B + \frac{p}{eB^2}\nabla\times\vec{B}. \tag{2}$$

With the assumption of 1/R variation of B field where R is the major radius in tokamak, ∇×B becomes zero. In the B2SOLPS5.0 code, the ∇p drift was replaced by the ∇B drift [1]. Since, however, B2SOLPS requires the numerical diffusive correction term to provide the numerical stability and this numerical diffusion term is hV where h is the cell size and V is the convective velocity, the large radial ∇B drifts in the upper and lower parts of the flux surfaces can generate the large numerical diffusion term resulting in the incorrect radial density profile [1]. In the B2SOLPS5.2, V. Rozhansky *et al*. [1] proposed the following form of the effective velocity that can replace the ∇B drift without giving the large value of the numerical diffusion term:

$$\text{new diamagnetic velocity} = \left(1-\frac{B^2}{\langle B^2\rangle}\right)\frac{1}{enB^2}\vec{B}\times\nabla p,$$
$$\text{where } \langle B^2\rangle = \frac{\int_{\text{inner boundary}}^{\text{separatrix}}\left(\oint B^2\sqrt{g}\,dx\right)dy}{\int_{\text{inner boundary}}^{\text{separatrix}}\left(\oint \sqrt{g}\,dx\right)dy}. \tag{3}$$

UEDGE employs the ∇B drift instead of the ∇p drift for the numerical accuracy and doesn't require the numerical diffusive term for the numerical stability purpose since it employs the fully implicit algorithm.

In this paper, the results of three cases were compared. The first case is the original UEDGE meaning without the numerical diffusive term, the second case is the UEDGE with the new formulation of B2SOLPS5.2 meaning the numerical diffusive term is calculated from the convective velocity using the new 'diamagnetic' velocity, and the third case is the UEDGE with the numerical diffusive term which is calculated from the convective velocity including the ∇B drift.

3. Simulation results

3.1 Comparison of the three cross-field drift algorithms

In the comparison, the case 1 is the results of the original UEDGE without the numerical diffusive term, the case 2 is the results of the UEDGE with the numerical diffusive term of the B2SOLPS5.2 using the new 'diamagnetic' velocity and the case 3 is the results of the UEDGE with the numerical diffusive term of the B2SOLPS5.0 using the ∇B drift. The comparison of the convergence is shown in fig. 1. In the plot, x axis is the power in MW and y axis is the minimum value of physical diffusion coefficient. Fig. 2 shows the examples of the physical diffusion coefficient having D_{min} = 0.3 and 0.1. In fig. 1, all three cases show less convergence as increasing the power and decreasing the D_{min}. In the figure, the dashed (case 1), solid (case 2), and dot (case 3) lines show the domain of the convergence for the each cross-field drift algorithm. The case 3 shows the best convergence among three cases. However, the accuracy is the different story. For example, the fig. 3 shows the ratio of the error in diffusion coefficient for the power 1.5 MW and D_{min} 0.3 where all three cases converged. The error is defined by the ratio of D-D_{phys} to D_{phys} where D is the diffusion coefficient defined by

$$D = \sqrt{D_{phys}^2 + D_a^2}, \quad D_a = hV, \tag{4}$$

where h is the mesh cell size and V is the drift velocity. Fig. 3 (a) shows the error in diffusion coefficient at the midplane and fig. 3 (b) shows at the top of the flux surface. In both locations, the case 2 using the new formula for the 'diamagnetic' velocity gives much smaller errors than the case 3. Especially, at the top of the flux surfaces, the case 3 shows the huge numerical diffusion coefficient about 2 times larger than the physical diffusion coefficient inside the separatrix but the new formulation of the drift in B2SOLPS5.2 significantly reduced the error in diffusion coefficient [1]. However, the case 2 shows the less convergence than the case 1 and 3 in fig. 1. Therefore, the new 'diamagnetic' velocity gives the huge benefit to the SOLPS which requires the diffusive term for the stability [1] but doesn't give the benefit to the UEDGE for the accuracy. The case 2 shows the better convergence than case 1 in fig. 1

meaning the numerical diffusive term improves the convergence of UEDGE with the sacrifice of the accuracy. Fig 4 shows (a) the electron density and (b) electron temperature of case 1 and 3 at the top of the flux surface where the large numerical diffusion term exists in case 3 with the power 2 MW and D_{min} 0.1. Fig 4 (b) shows the discrepancy of the temperature inside the separatrix due to the large numerical diffusive term. However, since the numerical diffusive term is artificial, it can be controlled by limiting the maximum value. Fig. 5 shows the decrease of the numerical diffusive term by limiting the maximum value of it to some fraction of the physical diffusion coefficient. The solid line doesn't have the limiting value, the dashed line has the 50% of the D_{phys}, the dot line has the 10% of the D_{phys}, and the dashed dot line has the 5% of D_{phys} as the limiting value. As in fig. 5, the numerical diffusive term can be decreased and in some cases, it can become zero.

3.2 Simulation results for the DIII-D shot 118898

Fig. 6 shows the simulation results of the UEDGE (solid line) and the experimental results of DIII-D 118898 (dashed line). The UEDGE with the numerical diffusive term of B2SOLPS5.2 failed to converge and UEDGE with the numerical diffusive term of B2SOLPS5.0 converged in this particular case. Fig. 6 (a) is the density profile and fig. 6 (b) is the electron temperature at the midplane. Previous version of UEDGE had failed to converge on this DIII-D 118898 after various attempts even with relatively large transport coefficients [5]. The new UEDGE converged with small and radially varying transport coefficients after using new features of UEDGE giving well-matched simulation results with experiment data, especially the density profile inside the separatrix.

4. Conclusions

Three cross-field drift algorithms were tested. The new algorithm of B2SOLPS5.2 reduced the numerical diffusive term compared B2SOLPS5.0 algorithm but didn't help UEDGE converge since UEDGE doesn't need the numerical diffusive term. However, the addition of numerical diffusive term to UEDGE increased the domain of the convergence with sacrifice of the accuracy and the error due to the existence of the numerical diffusive term could be reduced by limiting the maximum value of it. New UEDGE produced the experimental data of electron density and temperature of DIII-D 118898, which was unsuccessful to converge with the previous UEDGE.

Acknowledgements

The authors are grateful to Kaveeva Elizaveta and Vladimir Rozhansky for much advice in helping us understand the new scheme of SOLPS. This work was done under the auspices of the U.S. Department of Energy by Lawrence Livermore National Security, LLC, Lawrence Livermore National Laboratory under the contract DE-AC52-07NA27344

References

[1] V. Rozhansky, E. Kaveeva, P. Molchanov, I. Veselova, S. Voskoboynikov, D. Coster, G. Counsell, A. Kirk, S. Lisgo, the ASDEX-Upgrade Team and the MAST Team, Nucl. Fusion 49 (2009) 025007.

[2] G. J. Radford, A. V. Chankin, G. Corrigan *et al*. Contrib. Plasma Phys. 36 (1996) 187.

[3] T. D. Rognlien, G. D. Porter, and D. D. Ryutov J. Nucl. Mater. 266-269 (1999) 654.

[4] A. V. Chankin J. Nucl. Mater. 241-243 (1997) 199.

[5] Private communication with Gary Porter.

Figure captions

Fig. 1. Convergence domains of the cross-field drift algorithms.

Fig. 2. Examples of the physical diffusion coefficient, D_{phys} and D_{min}.

Fig. 3. Error in diffusion coefficients (a) at the midplane and (b) at the top.

Fig. 4. (a) The electron density and (b) electron temperature of case 1 and case 3 at the top.

Fig. 5. Progressively limiting the maximum value of the numerical diffusive term gives another solution method.

Fig. 6. Comparison of UEDGE with DIII-D shot# 118898. (a) The electron density and (b) electron temperature.

Figures

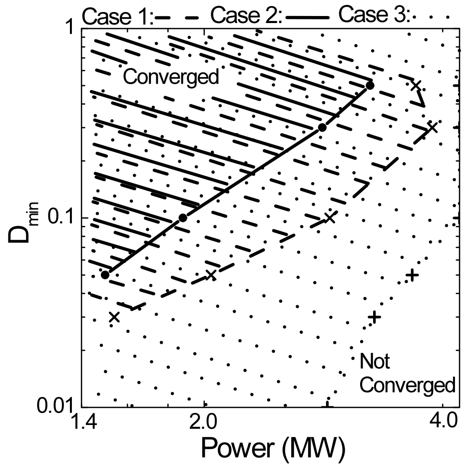

Fig. 1

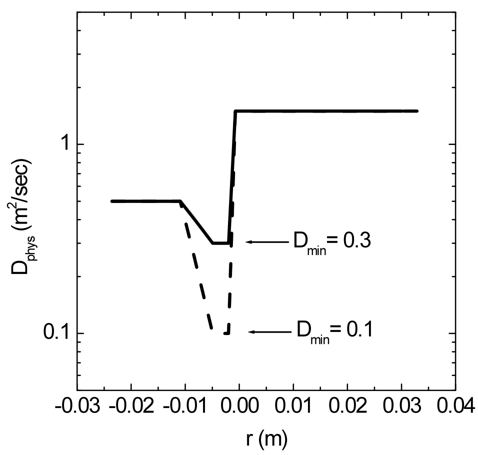

D_{phys} (m^2/sec)
1
0.1
D_{min} = 0.3
D_{min} = 0.1
-0.03 -0.02 -0.01 0.00 0.01 0.02 0.03 0.04
r (m)

Fig. 2

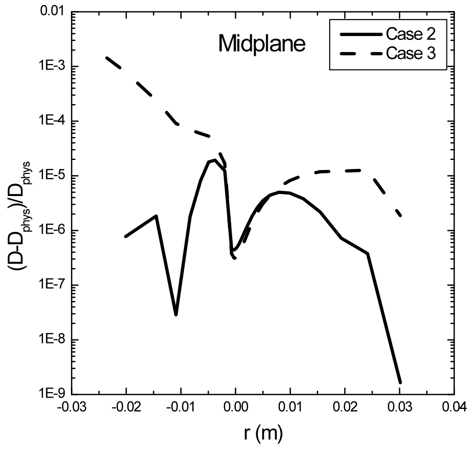
Midplane
Case 2
Case 3
(D-D$_{phys}$)/D$_{phys}$
r (m)

(a)

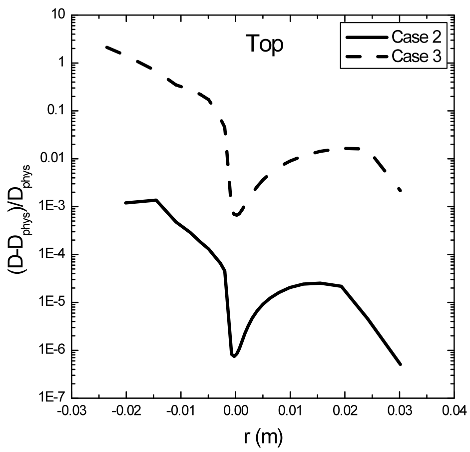
Top
Case 2
Case 3
(D-D$_{phys}$)/D$_{phys}$
r (m)

(b)

Fig. 3

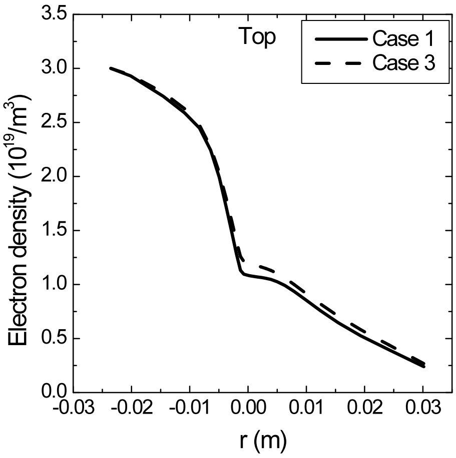
Top
Case 1
Case 3
Electron density ($10^{19}/m^3$)
r (m)
3.5
3.0
2.5
2.0
1.5
1.0
0.5
0.0
-0.03
-0.02
-0.01
0.00
0.01
0.02
0.03

(a)

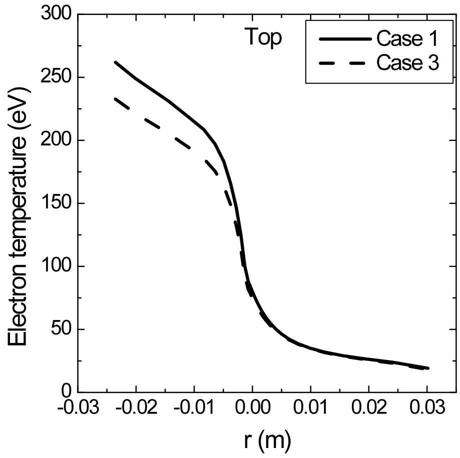
Top
Case 1
Case 3
Electron temperature (eV)
r (m)
300
250
200
150
100
50
0
-0.03
-0.02
-0.01
0.00
0.01
0.02
0.03

(b)

Fig. 4

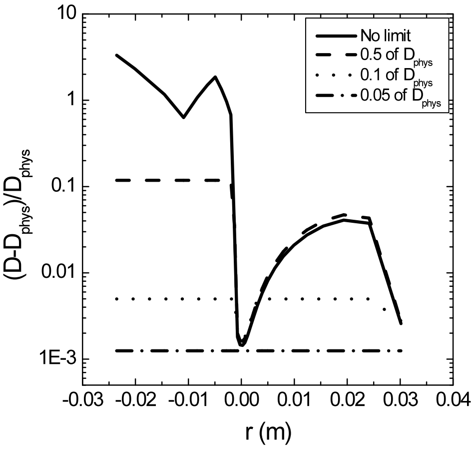

10
1
0.1
0.01
1E-3
(D-D_phys)/D_phys
-0.03 -0.02 -0.01 0.00 0.01 0.02 0.03 0.04
r (m)
No limit
0.5 of D_phys
0.1 of D_phys
0.05 of D_phys

Fig. 5

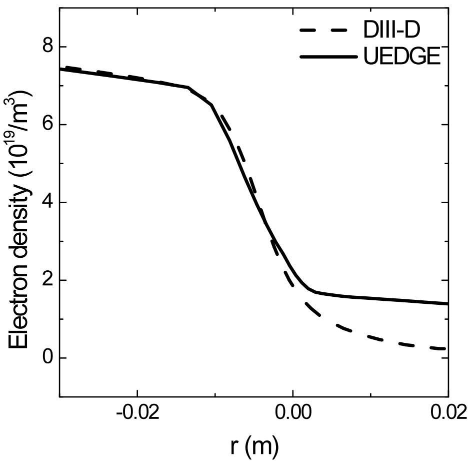
DIII-D
UEDGE
Electron density ($10^{19}/m^3$)
r (m)
0
2
4
6
8
-0.02
0.00
0.02

(a)

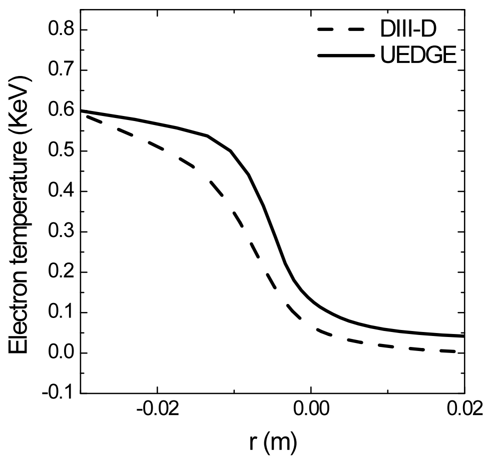
DIII-D
UEDGE
Electron temperature (KeV)
r (m)
-0.1
0.0
0.1
0.2
0.3
0.4
0.5
0.6
0.7
0.8
-0.02
0.00
0.02

(b)

Fig. 6